agriculture

IMPACT FACTOR 3.408

CITESCORE 3.1

Article

# New Spectral Index and Machine Learning Models for Detecting Coffee Leaf Miner Infestation Using Sentinel-2 Multispectral Imagery

Emerson Ferreira Vilela, Williams Pinto Marques Ferreira, Gabriel Dumbá Monteiro de Castro, Ana Luísa Ribeiro de Faria, Daniel Henrique Leite, Igor Arantes Lima, Christiano de Sousa Machado de Matos, Rogério Antonio Silva and Madelaine Venzon

Special Issue

Sustainable Pest Management for Coffee Production

Edited by

Prof. Dr. Madelaine Venzon and Prof. Dr. Angelo Pallini

MDPI

https://doi.org/10.3390/agriculture13020388

*agriculture*

MDPI

*Article*

# New Spectral Index and Machine Learning Models for Detecting Coffee Leaf Miner Infestation Using Sentinel-2 Multispectral Imagery

**Emerson Ferreira Vilela [1], Williams Pinto Marques Ferreira [2], Gabriel Dumbá Monteiro de Castro [3], Ana Luísa Ribeiro de Faria [4], Daniel Henrique Leite [5], Igor Arantes Lima [6], Christiano de Sousa Machado de Matos [7], Rogério Antonio Silva [7] and Madelaine Venzon [1,*]**

[1] Agriculture and Livestock Research Enterprise of Minas Gerais (EPAMIG-Sudeste), Viçosa 36570-000, MG, Brazil
[2] Brazilian Enterprise for Agricultural Research (EMBRAPA), Viçosa 36570-000, MG, Brazil
[3] Department of Agricultural Engineering, Federal University of Viçosa, Viçosa 36571-900, MG, Brazil
[4] Department of Geography, Federal University of Viçosa, Viçosa 36570-900, MG, Brazil
[5] Department of Agronomy, Federal University of Viçosa, Viçosa 36570-900, MG, Brazil
[6] Department of Food Science, Federal University of Lavras, Lavras 37200-000, MG, Brazil
[7] Agriculture and Livestock Research Enterprise of Minas Gerais (EPAMIG-Sul), Lavras 37200-970, MG, Brazil
* Correspondence: madelaine@epamig.br

**Abstract:** The coffee leaf miner (*Leucoptera coffeella*) is a key coffee pest in Brazil that can cause severe defoliation and a negative impact on the productivity. Thus, it is essential to identify initial pest infestation for the sake of appropriate time control to avoid further economic damage to the coffee crops. A fast non-destructive method is an important tool that can be used to monitor the occurrence of the coffee leaf miner. The present work aims to identify the occurrence of coffee leaf miner infestation through a new vegetation index, using multispectral images from the Sentinel-2 satellite and the Google Earth Engine platform. Coffee leaf miner infestation was measured in the field in four cities in the state of Minas Gerais. The largest infestations occurred in September, October, and November but particularly in October 2021, in which the rate of infestation reached 85%, followed by September 2020 with a maximum infestation of 76%. The calculation steps of the vegetation indices and mappings were carried out in the Google Earth Engine cloud processing platform through the development of a script in JavaScript programming language. Combinations of two sensitive bands were selected to detect coffee leaf miner infestation, and from these, the "Coffee-Leaf-Miner Index" was developed, which was compared with other existing vegetation indices in terms of their performance for coffee leaf miner detection. The combination of the NIR–BLUE and NIR–RED bands was more sensitive for the detection of coffee leaf miner infestation; therefore, the NIR, BLUE, and RED bands were selected to develop the new index. The "Coffee-Leaf-Miner Index" presented the best performance among those evaluated, with a coefficient of determination of about 0.87, a root mean square error of 4.92% coffee leaf miner infestation, accuracy of 89.47%, and kappa coefficient of 95.39. The $R^2$ range of other spectral indices which exist in the literature and which were used in this study was from 0.017 to 0.867, and the root mean square error ranged from 4.996 to 13.582% coffee leaf miner infestation. The machine learning method was then adopted using the supervised Random Forest and Support Vector Machine algorithms to recognize patterns of coffee leaf miner infestation in the field, only the Coffee-Leaf-Miner Index was used for the identification test of the coffee leaf miner infestation. The Support Vector Machine with linear Kernel type was applied to establish a discrimination model. The number of trees for the Random Forest classifier was 100. The Support Vector Machine presented a lower performance than the Random Forest algorithm, but the performance of both were above 80% for user and producer precision. Three bands (Blue, Red, NIR) were selected for the creation of the new index, which showed capacity for remote detection of coffee leaf miner infestation on a regional scale. Thus, "Coffee-Leaf-Miner Index" can identify coffee leaf miner infestation thanks to all the complexity involved in detecting pests via orbital remote sensing.



**Citation:** Vilela, E.F.; Ferreira, W.P.M.; Castro, G.D.M.d.; Faria, A.L.R.d.; Leite, D.H.; Lima, I.A.; Matos, C.d.S.M.d.; Silva, R.A.; Venzon, M. New Spectral Index and Machine Learning Models for Detecting Coffee Leaf Miner Infestation Using Sentinel-2 Multispectral Imagery. *Agriculture* **2023**, *13*, 388. https://doi.org/10.3390/agriculture13020388

Academic Editor: Xiuliang Jin

Received: 19 December 2022
Revised: 28 January 2023
Accepted: 31 January 2023
Published: 6 February 2023

**Keywords:** Google Earth Engine; *Leucoptera coffeella*; machine learning

## 1. Introduction

Brazil is the world's largest coffee producer, and it is responsible for one-third of world production [1]. Most of the national production of Arabica coffee is in the state of Minas Gerais, which is responsible for about 70% of the country's production [2]. In this context, coffee farming is an important economic activity for agribusiness and small farmers in Minas Gerais and, consequently, also for Brazil. However, one of the factors that can negatively affect coffee production is pest attacks that occur during coffee production. Therefore, measures that can contribute to monitoring pest development are of fundamental importance.

The coffee leaf miner *Leucopetra coffeella* (Lepitoptera: Lyonetiidae) is the main pest of Arabica coffee in Brazil [3]. The pest has a widespread occurrence in Minas Gerais and attacks the leaves of the coffee plant, causing necrosis and defoliation of up to 75% and losses in production that can exceed 50% [4,5]. Crops that are severely defoliated in the drought as a consequence of coffee leaf miner infestation take about two years to recover [6] and can cause hundreds of millions of dollars in losses [7]. The increase in coffee leaf miner infestation is associated with several factors, such as indiscriminate use of insecticides, the presence of extensive crops or large areas of continuous monoculture planting, coffee planting in larger spacings, high temperature, prolonged dry periods, and low relative humidity, as well as the absence of natural enemies due to lack of resources in monocultures [6,8]. Its most serious occurrence is associated with higher temperatures [9] and the driest period of the year [5]. In Minas Gerais, the increase in infestation starts in July/August, with a peak in October [10].

Monitoring the coffee crop is an important practice for crop phytosanitary management, as it allows the producer to know when there is an infestation of coffee leaf miner and makes it possible to decide whether or not to carry out the control measures. Alternative, efficient, and low-cost methods that can monitor large areas with an infestation of pests and diseases in crops have been gaining prominence with the use of remote sensing [11–13]. Such methods are based on the different spectral responses between a healthy plant and one with a pest or disease [14]. These spectral responses may, for example, be due to changes in morphology, leaf color, chlorosis, and necrosis. For the analysis of the spectral response over time, it is necessary to select and process a large number of images, which is often time-consuming. Therefore, it was necessary to create platforms that would allow these analyses to be streamlined.

For the processing of a large amount of geospatial data (geo-big data), some platforms have emerged. Such platforms include Amazon Web Services (AWS), which was launched in 2006, and Microsoft Corporation's Azure platform, which was launched in 2010; both of these platforms are paid [15]. In 2010, Google launched the free cloud computing platform (Google Earth Engine—GEE) that allows quick access and processing of various sets of remote sensing data. The GEE provides access to a global remote sensing database spanning four decades and receives around 4000 new datasets daily in its database [16]. This amount of data allows the temporal analysis of the coffee crop in any region of the world, and among the databases that are available in the GEE is the collection of Sentinel satellites; machine learning algorithms (M.L.) are among the available tools [15]. Several studies have used the GEE for fast, regional, and accurate monitoring, e.g., the mapping of infestation by *Spodoptera frugiperda* in maize [17], the analysis of Fulsarium in the culture of wheat [11], and the evaluation of the impacts of chilling injury on soybean [18].

Sentinel-2 was released in 2015 and features an MSI multispectral sensor with 13 spectral bands. The visible (RGB) and Infrared (NIR) bands have a spatial resolution of 10 m and a revisit period of about 5 days [19]. Thus, monitoring can be carried out in short periods and with precision at the level of small rural properties. The M.L. can be defined as

a branch of artificial intelligence that considers that the system can learn from data, detect patterns, and make decisions with minimal human intervention [20]. In recent years, M.L. has gained prominence as an important tool in remote sensing and precision agriculture and has been used to assist in the identification of diseases and pests [11,21,22].

Several studies have been conducted using vegetation indices to detect pest/disease in different crops. Using the NDVI time series, images from Sentinel and the GEE, it was possible to monitor the infestation of Fall Armyworm (*Spodoptera frugiperda*) in corn [17]. Twenty vegetation indices found in the literature were used to evaluate the infestation of *Spodoptera frugiperda* in the sorghum crop, with the NDVI and LAI (Leaf Area Index) being the vegetation indices that presented the best performances to identify the infestation [12]. In another study, 63 vegetation indices associated with machine learning algorithms based on decision trees were used to assess coffee rust infestation [23]. Spectral reflectance analysis has also been considered to identify pest/disease. Using machine learning algorithms and Satellite Sentinel images, it was possible to separate areas of cotton under attack by *Spodoptera frugiperda* by considering the spectral reflectance [13]. Nine vegetative indices were evaluated to identify the damage caused by frost in coffee plantation areas, with the NDVI being the index that presented the best results for identifying and evaluating frost damage in coffee plants [24]. Few studies have proposed the creation of specific vegetation indices for a given pest/disease, e.g., a new vegetation index for discriminating yellow-rust-infected winter wheat [22]. Another index was created to detect Wheat Fusarium Head Blight Using Sentinel-2 Multispectral Imagery [11].

Vegetation indices common in the literature are not crop or pest/disease specific and cannot, by themselves, discriminate crop-specific parameters. Therefore, it would be important to create specific indices to identify coffee leaf miner infestation. There is no specific vegetative index in the literature to identify leaf miner infestation.

The present work aimed to select the combination of two Sentinel-2 bands to identify the levels of coffee leaf miner infestation in coffee crops; develop a new index to estimate coffee leaf miner infestation in coffee crops; and map the coffee leaf miner attack infestation in coffee crops using Sentinel-2 images through the Google Earth Engine platform.

## 2. Materials and Methods

### *2.1. Study Area*

The study was carried out at the Experimental Research Stations of Agriculture and Livestock Research Enterprise of Minas Gerais (Epamig), which are located in the cities of Três Pontas (CETP), São Sebastião do Paraíso (CESP), Machado (CEMA), and Patrocínio (CETP), in the state of Minas Gerais (Figure 1).

The coffee cultivars and edaphoclimatic characteristics of the experimental research station for the years 2019 to 2021 are described in Table 1, with precipitation data obtained from the Climate Hazards Group InfraRed Precipitation with Stations (CHIRPS) database [25] and the temperature data obtained from the database of the Latest Climate Reanalysis Produced by ECMWF/Copernicus Climate Change Service—ERA 5 [26].

**Table 1.** Coffee cultivars and edaphoclimatic characteristics of the experimental research stations.

| Characteristics | CETP | CESP | CEMA | CEPC |
|---|---|---|---|---|
| Cultivar | Mundo Novo | Catuaí 99 | Catuaí 99 | Rubi |
| Elevation (m) | 916 | 880 | 970 | 997 |
| Average annual rainfall (mm) | 720 | 857 | 816 | 845 |
| Annual average temperature (°C) | 21.4 | 22 | 21.5 | 21.7 |
| Latitude (S) | 21°20′37.014″ | 20°54′42.023″ | 21°40′50.848″ | 18°59′28.284″ |
| Longitude (W) | 45°28′59.452″ | 47°7′20.341″ | 45°56′38.069″ | 46°59′21.700″ |

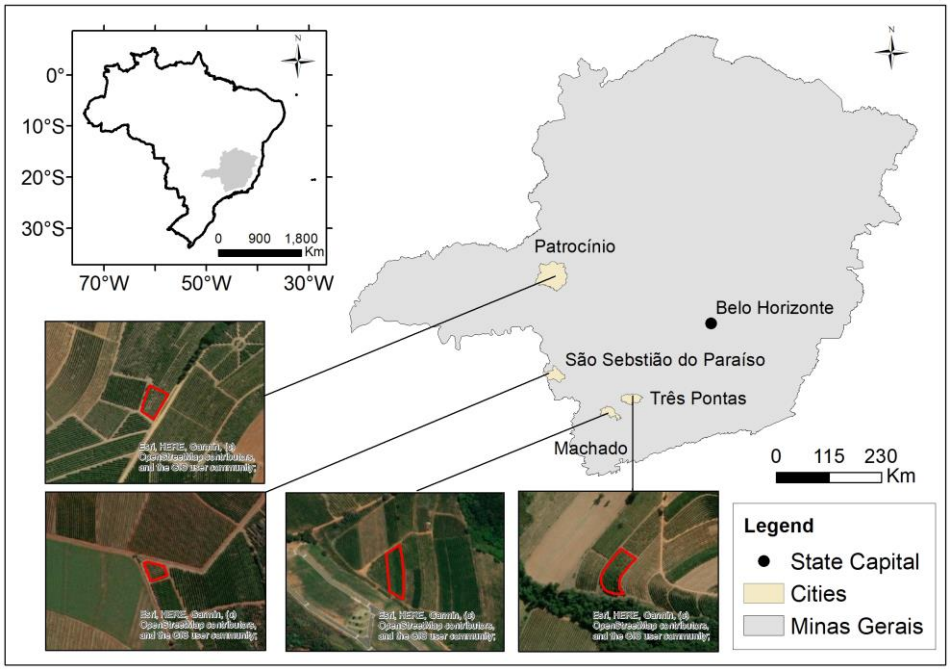


**Figure 1.** Experimental Research Station where coffee leaf miner infestation levels were monitored: Três Pontas (CETP), São Sebastião do Paraíso (CESP), Machado (CEMA), and Patrocínio (CEPC).

In each experimental research station, a plot with the following areas was selected: CETP (2575 $m^2$); CESP (930 $m^2$); CEMA (2279 $m^2$); and CEPC (1609 $m^2$). Although the spatial resolution of the Sentinel-2A satellite is 10 m for bands 2, 3, 4, and 8 and 20 m for bands 5, 6, and 7, the plot areas were enough to meet the resolution of Sentinel-2A (Table 2).

**Table 2.** Spectral bands and resolution of the Sentinel-2A sensor MSI.

| | Spectral Band | Central Wavelength (nm) | Bandwidth (nm) | Spatial Resolution (m) |
|---|---|---|---|---|
| B1 | Coastal aerosol | 443 | 20 | 60 |
| B2 | Blue | 490 | 65 | 10 |
| B3 | Green | 560 | 35 | 10 |
| B4 | Red | 665 | 30 | 10 |
| B5 | Red-edge 1 (Re1) | 705 | 15 | 20 |
| B6 | Red-edge 2 (Re2) | 740 | 15 | 20 |
| B7 | Red-edge 3 (Re3) | 783 | 20 | 20 |
| B8 | Near Infrared (NIR) | 842 | 115 | 10 |
| B8a | Red-edge 4 (Re4) | 865 | 20 | 20 |
| B9 | Water vapor | 945 | 20 | 60 |
| B10 | Shortwave Infrared/cirrus | 1.375 | 30 | 60 |
| B11 | Shortwave Infrared 1 | 1.610 | 90 | 20 |
| B12 | Shortwave Infrared 2 | 2.190 | 180 | 20 |

### *2.2. Data Collect*

The first step of the present work was the monthly monitoring of the coffee leaf miner infestation estimate (CLMIE) between January 2019 and December 2021. For the monitoring, leaves were randomly collected from 50 plants per plot. In each plant, from the leaves of the 3rd or 4th pair of two branches, on opposite sides, we collected four distal leaves located in the middle plant strata until the sample collection reached 200 leaves per plot. Only leaves with intact mines were considered for the miner count. We kept the coffee leaves in paper bags and later examined them in the laboratory to assess the active mines

(infestation). We calculated the coffee leaf miner (CLM) infestation rate using the following formula:

$$\text{CLM infestation rate } (\%) = \frac{\text{Number of coffee leaf with active mine} \times 100}{\text{Total number of collected coffee leaves}}$$

The second step was the selection of the months with the highest incidence of CLMIE. Then, the selection of Sentinel-2 multispectral images (Table 2) was carried out in three periods—i.e., on 2 September 2019, between 26 and 28 September 2020, and from September 20 to 21, 2021—to obtain the reflectance of bands in the coffee crop area from coffee leaf miner infestation. Coastal aerosol (B1), Near-Infrared (NIRn) (B8a), Water vapor (B9), Shortwave Infrared/cirrus (B10), Shortwave Infrared 1 (SWIR1) (B11), and Shortwave Infrared 2 (SWIR2) bands (B12) were not considered in the present study, as they were not part of the vegetation indices used in this study.

### *2.3. Vegetation Indices*

The geoprocessing steps and the calculation of the vegetation indices were carried out on the Google Earth Engine cloud processing platform through the development of a script in the JavaScript programming language. Using the geographical coordinates of the experimental research stations (Table 1), satellite images of the study areas for the months from 2019 to 2021 were obtained. Thus, with the spectral reflectance information available in the images, it is possible to obtain the average value of each one of the vegetation indices in each of the experimental research stations could be obtained.

Based on the spectral reflectance values of Sentinel satellite images obtained for September 2020 and 2021, in coffee crops with and without coffee leaf miner infestation, two basic vegetation indices were adopted, according to the methodology described by Liu et al. [11], i.e., difference vegetation index (DVI) [27] and ratio vegetation index (RVI) [28], as well as modifications of these two indices. These indices allowed us to assess which spectral bands are more sensitive to indicate infestation with coffee leaf miner.

Regression equations based on the variables vegetation indices and coffee leaf miner infestation were then developed. Through the regression equations, the spectral bands that best indicated the coffee leaf miner infestation in coffee crop areas were selected and then compared using statistical performance criteria (determination coefficient—$R^2$, root mean square error—RMSE). The same statistical criteria (RMSE and $R^2$) were used later to compare some vegetation indices described in the literature with the new index.

### *2.4. The New Index—CLMI*

From the selected spectral bands, a new vegetation index called Coffee-Leaf-Miner Index (CLMI) was generated to estimate coffee leaf miner infestation. The CLMI was based on the area covered by a triangle, as per the methodology described by [11]. To calculate the area of the triangle, a matrix formed by the reflectance values of the selected bands and the respective central wavelengths of these bands was generated. The area of the triangle was calculated by dividing the determinant of the matrix (Equation (1)).

$$\text{CLMI} = \text{ Triangle area} = \frac{\text{Determinant}}{2} \quad (1)$$

In this study, in addition to the new index, ten other relevant vegetation indices from the literature were selected (Table 3), and these were calculated through the spectral reflectance values of the Sentinel-2 satellite images. All 10 indices were compared with the CLMI to assess the coffee leaf miner infestation in coffee crops, through statistical performance criteria ($R^2$ and RMSE) considering the month of September from the years 2019 to 2021. Based on the results found for September, the 3 indices that presented the best performers (higher $R^2$ and lower RMSE) were compared to CLMI based on October data. All statistical analyses were performed using R 4.2.1 software (R Development Core Team, 2022) [29].

**Table 3.** Characteristics of the vegetation index used to monitor the coffee leaf miner in the experimental research station.

| Definition | Formula | Reference |
|---|---|---|
| Normalized Difference Vegetation Index (NDVI) | $\frac{NIR-RED}{NIR+RED}$ | [30] |
| Enhanced Vegetation Index (EVI) | $2.5 \times \frac{NIR-RED}{NIR+6\times RED-7.5\times BLUE+1}$ | [31] |
| Simple Ratio (SR) | $\frac{NIR}{RED}$ | [27] |
| Green Normalized Difference Vegetation Index (GNDVI) | $\frac{NIR-GREEN}{NIR+GREEN}$ | [32] |
| Infrared Percentage Vegetation Index (IPVI) | $\frac{NIR}{NIR+RED}$ | [33] |
| Modified Chlorophyll Absorption Ratio Index (MCARI) | $(RE1-RED)-(0.2\times(RE1-GREEN)))\times\frac{RE1}{RED}$ | [34] |
| MERIS Terrestrial Chlorophyll Index (MTCI) | $\frac{NIR-RE1}{RE1-RED}$ | [35] |
| Red Edge Inflection Point (REIP) | $700+35\times\frac{\frac{NIR+RED}{2}-RE1}{RE2-RE1}$ | [36] |
| Plant Senescence Reflectance Index (PSRI1) | $\frac{RED-GREEN}{RE1}$ | [37] |
| Soil-Adjusted Vegetation Index (SAVI) | $\frac{(1+L)\times(NIR-RED)}{(NIR+RED+L)}$ | [38] |

### *2.5. Index Test (CLMI) for Mapping Coffee Leaf Miner Infestation*

The mapping step was carried out on the Google Earth Engine platform through the development of a script in the JavaScript programming language.

The coffee leaf miner infestation was mapped using the CLMI index on Sentinel-2A images, which were from 26 to 28 September 2020, from four plots in the CETP, CESP, CEMA, and CEPC experimental research stations.

Given that the coffee leaf miner infestation dynamics are influenced by precipitation, the average precipitation values from April to May from the Climate Hazards Group Infrared Precipitation with Station (CHIRPS) data were used. However, the addition of this variable did not show satisfactory results. Thus, only the CLMI was used for the identification test of the coffee leaf miner infestation.

The machine learning method was then adopted using the supervised Random Forest (RF) and Support Vector Machine (SVM) algorithms to recognize patterns of coffee leaf miner infestation in the field based on the images obtained in the four plots (CETP, CESP, CEMA, CEPC) to train the algorithm to recognize the coffee leaf miner infestation using CLMI.

These two machine learning methods (RF and SVM) are among the most popular algorithms used in classification and regression, and they are characterized by similar high performance [39]. The SVM algorithm, which was first introduced in the late 1970s, is one of the most widely used kernel-based learning algorithms in a range of machine learning applications, in particular, image classification. SVM, in its basic form, is a linear binary classifier which identifies a single boundary between two classes [39].

The RF is a set of learning algorithms, which were proposed by Breiman [40] and which consist of a set of decision trees and independent and identically distributed random vectors. SVM and RF can handle learning tasks with a small amount of training datasets but demonstrate competitive results.

In this study, SVM with linear kernel type was applied to establish a discrimination model. For Random Forest, the number of decision trees to create was 100. The confusion matrix was used to assess the accuracy of supervised algorithms. Specifically, before training the algorithm, 30% of the pixels of all plot images were reserved to validate the training of the algorithms (Random Forest and SVM) in the prediction of CLMIE. The remaining pixels (70%) were used to train the algorithms.

The confusion matrix was extracted based on the 30% of data reserved for validation. The CEMA plot was used to represent a healthy plot, as it had the lowest infestation (8% infestation). The other stands were considered infested with coffee leaf miner infestation above 20%.

## 3. Results

### *3.1. Field Monitoring*

The monthly monitoring of the occurrence of coffee leaf miner infestation between January 2019 and December 2021 in CETP, CESP, CEMA, CEPC are presented in Table 4.

**Table 4.** Maximum and the average percentage of coffee leaf miner infestation in Três Pontas, São Sebastião, Machado, and Patrocínio during the period from 2019 to 2021. M = Maximum; A = Average.

| | 2019 | | | 2020 | | | 2021 | | | Total | |
|---|---|---|---|---|---|---|---|---|---|---|---|
| | Date | M | A | Date | M | A | Date | M | A | M | A |
| | | % | | | % | | | % | | % | |
| January | 29 | 5 | 2.0 | 20 | 23 | 9.1 | 1 | 1 | 0.4 | 23 | 6.8 |
| February | 25 | 13 | 5.6 | 17 | 5 | 3.1 | 22 | 3 | 1.3 | 13 | 5.2 |
| March | 4 | 8 | 4.1 | 9 | 1 | 0.4 | 5 | 7 | 3.3 | 8 | 4.0 |
| April | 24 | 8.5 | 4.9 | 1 | 17 | 7.8 | 26 | 8 | 3.5 | 17 | 8.3 |
| May | 13 | 1 | 0.7 | 7 | 13.5 | 4.8 | 17 | 13 | 4.1 | 13.5 | 6.2 |
| June | 10 | 0.5 | 0.2 | 8 | 27 | 12.3 | 21 | 35 | 16.3 | 35 | 15.2 |
| July | 31 | 5 | 2.3 | 29 | 27.5 | 10.9 | 27 | 32 | 9.6 | 32 | 14.6 |
| August | 12 | 1.5 | 0.7 | 31 | 30 | 18.5 | 17 | 29 | 10.0 | 30 | 14.9 |
| September | 2 | 3 | 2.7 | 28 | 76 | 32.3 | 20 | 46 | 20.0 | 76 | 30.0 |
| October | 4 | 30 | 24.0 | 19 | 56 | 23.0 | 18 | 85 | 31.5 | 85 | 41.6 |
| November | 15 | 19 | 17.3 | 16 | 56 | 18.9 | 23 | 17 | 7.8 | 56 | 22.7 |
| December | 15 | 14.5 | 10.2 | 7 | 8.5 | 7.3 | 13 | 12.5 | 7.5 | 14.5 | 10.1 |

The occurrence of coffee leaf miner in coffee plantations can be observed throughout the months of the year (Table 4). However, from June onwards, there was an increase in coffee leaf miner infestation, with the largest infestations occurring in September, October, and November but particularly in October 2021, in which the infestation reached up to 85%, followed by September 2020 with a maximum infestation of 76%. The lowest infestations were in February and March (Table 4).

### *3.2. Spectral Characteristics of the Coffee Crop with Coffee Leaf Miner*

Considering that the month of September was the month with the second highest incidence of coffee leaf miner in the study region, as well as the month with the highest number of images available, the month of September of the years 2019, 2020, and 2021 was then considered to create of the new index.

Figure 2 shows the spectral reflectance in coffee crops with different levels of coffee leaf miner infestation from the image obtained on 26 and 28 September 2020.

Based on the pattern of the spectral curve, it is possible to identify that the CETP coffee crop that showed the lowest reflectance in the Near Infrared region (NIR) and the highest reflectance in the Blue wavelength region was the one with the highest coffee leaf miner infestation. In the Red region, it is observed that the higher the percentage of leaf miner infestation (8%; 21.5%; 23.5%, and 76%), the greater the reflectance.

Comparing the reflectance of the coffee crop with the highest infestation (CETP—76%) with the one with the lowest infestation (CEMA—8%) in the NIR region, it can be seen that the higher the infestation, the lower the reflectance.

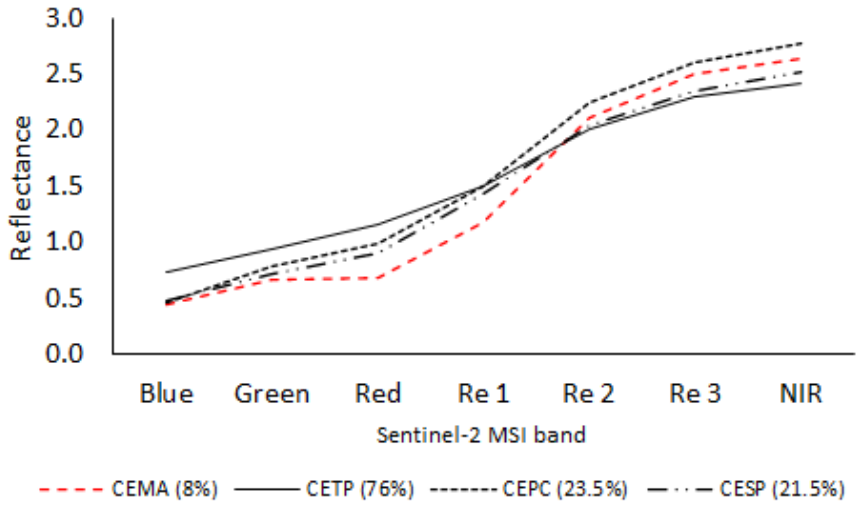


**Figure 2.** Multispectral reflectance average of the image obtained on 26 and 28 September 2020 of coffee crops with different levels of coffee leaf miner infestation.

### *3.3. Index Development*

Based on the coefficient of determination ($R^2$) and the Root Mean Square Error (RMSE) (Figure 3), which were obtained for the 24 regression equations based on the difference or ratio of band wavelengths and the level of coffee leaf miner infestation recorded in the field, the bands that best show coffee leaf miner infestation in coffee crops areas were selected.

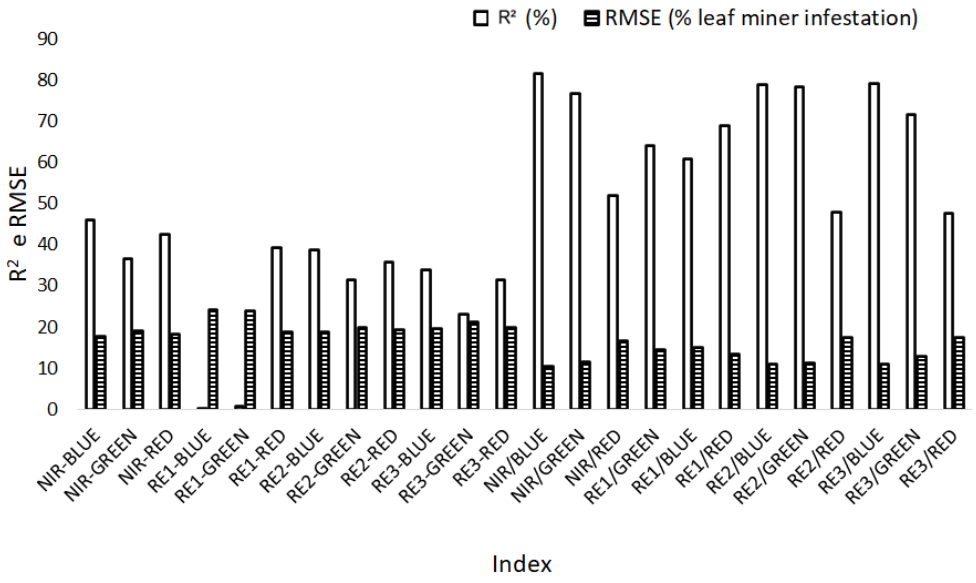


**Figure 3.** Root mean error square (RMSE) percentage coffee leaf miner infestation and percentage of coefficient of determination ($R^2$) of the models developed using the basic vegetation index and its modifications.

Given the analysis of the ratio between the different bands considered, although the indices based on the ratio (NIR/BLUE and RE3/BLUE) have presented the best results because of the grouping of the values of higher $R^2$ and lower RMSE (Figure 3), the CLMI index based on the NIR, RE3, and BLUE bands did not present a good performance for the CLMIE, because of the low values of $R^2$ and high values of RMSE. Therefore, the indices based on the difference between the bands were also analyzed, with the NIR-BLUE and NIR-RED differences being those that presented the best performances because of the higher $R^2$ and lower RMSE. The NIR, RED, and BLUE bands were then selected.

Thus, from the analysis of the area of the triangle, which was formed by the values of the spectral reflectance of the NIR, RED, and BLUE (Figure 4), the CLMI index was developed for the CLMIE.

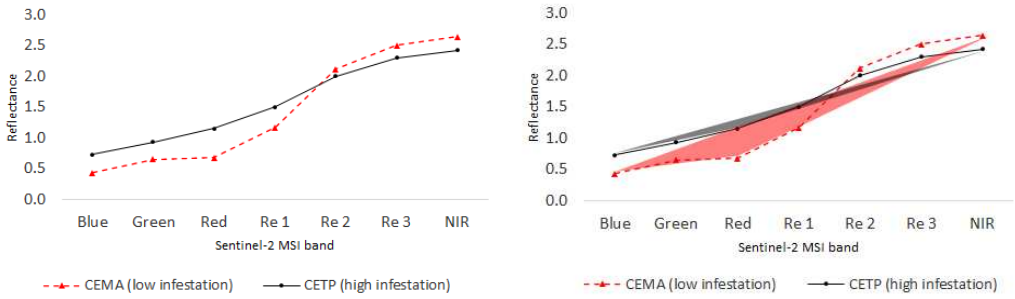


**Figure 4.** Overview of the reflectance of the image obtained on 28 September 2020 (**a**) and the area of the triangle based on the reflectance values of Blue, Red, and Near Infrared (NIR) (**b**) for coffee crops with low and high coffee miner infestation. Low infestation = 8%, and high infestation = 76%.

Based on the area of the triangle formed in Figure 4, the CLMI index was created from Equation (2).

$$\text{CLMI} = \frac{(842 - 490) \times (\text{RED} - \text{BLUE}) - (665 - 490) \times (\text{NIR} - \text{BLUE})}{2} \quad (2)$$

where RED, BLUE, and NIR are the reflectance values of the bands, and the numbers 665, 490, and 842 are the central wavelengths of the same bands (Table 2).

Still based on Figure 4, it is noteworthy that the smaller the area of the triangle formed, the greater the level of coffee leaf miner infestation because coffee leaf miner infestation decreases the reflectance in the NIR region and increases the reflectance in the Blue region; therefore, the lower the value of the CLMI index, the greater the level of infestation by coffee leaf miner in the coffee crops.

### *3.4. Estimation of Coffee Leaf Miner Infestation Using Simulation with Multispectral Data*

The CLMI index was compared with 10 other relevant vegetation indices in the literature to identify coffee leaf miner infestation in coffee crops using statistical performance criteria ($R^2$ and RMSE). For a better adjustment of the generated models, the extreme values were removed, i.e., 0% of infestation and 76% of leaf miner infestation. Table 5 summarizes the $R^2$ and RMSE values found in the developed models of the CLMI and the ten relevant vegetation indices in the literature.

The CLMI presented the best $R^2$ and RMSE values of 0.869 and 4.94, respectively. The new index was the best index to identify coffee leaf miner infestation. The existing vegetation indices in the literature that presented the best performance to identify coffee leaf miner infestation were NDVI, IPVI, EVI, and SAVI, which presented an $R^2$ above 0.85 and an RMSE below 5.5. The vegetation indices that presented a low performance for identifying the leaf miner infestation were the MTCI and REIP, which presented with an R2 below 0.4 and an RMSE above 11.

Figure 5 also shows, based on the results of the models, the estimated values of the coffee leaf miner infestation and those measured in the field in the period between 26 and 28 September 2020.

**Table 5.** $R^2$ and RMSE (% coffee leaf miner infestation) of models to estimate coffee leaf miner infestation, as developed from the CLMI and the 10 vegetation indices for September from the years 2019 to 2021.

| Indices | $R^2$ | RMSE |
|---|---|---|
| CLMI | 0.869 | 4.942 |
| NDVI | 0.867 | 4.996 |
| IPVI | 0.865 | 5.036 |
| EVI | 0.859 | 5.142 |
| SAVI | 0.838 | 5.517 |
| GNDVI | 0.785 | 6.349 |
| PSRI1 | 0.744 | 6.931 |
| SR | 0.659 | 8.002 |
| MCARI | 0.640 | 8.219 |
| MTCI | 0.302 | 11.449 |
| REIP | 0.017 | 13.582 |

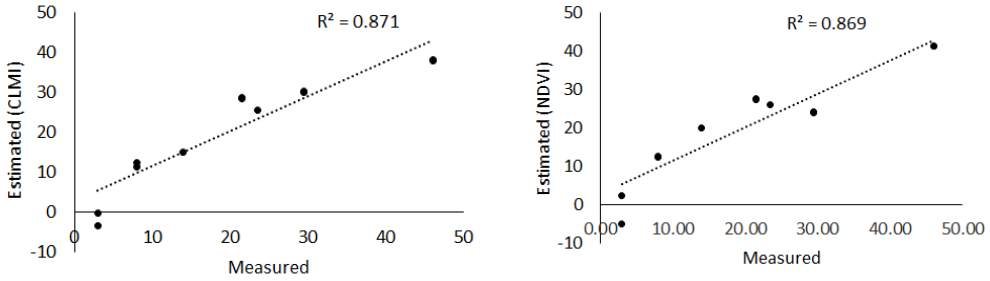


(**a**) (**b**)

**Figure 5.** Relationship between the measured in the field and the one estimated from the New Index (**a**) and NDVI (**b**) for coffee crops with different levels of coffee leaf miner infestation in the period between 26 and 28 September 2020.

Figure 5 shows the scatter plots between the estimated coffee leaf miner infestation and that measured in the field. It can be observed that the generated models had difficulties in identifying low leaf miner infestations, reaching negative values when the leaf miner infestation was low.

The vegetation indices that had the highest $R^2$ value (>0.85) and the lowest RMSE (<5.5) (Table 5) for the CLMIE in September were used for the CLMIE in October of the years 2019 and 2020 (Table 6), because in October 2021, there were no cloud-free satellite images of the studied locations. October was the month with the highest infestation of coffee leaf miner (Table 4).

**Table 6.** $R^2$ and RMSE of models to estimate coffee leaf miner infestation, developed from the CLMI and the 3 vegetation indices for October from the years 2019 to 2020.

| Indices | $R^2$ | RMSE |
|---|---|---|
| CLMI | 0.568 | 3.841 |
| IPVI | 0.563 | 3.861 |
| EVI | 0.556 | 3.892 |
| NDVI | 0.554 | 3.902 |

For October, the CLMI was the best index to estimate coffee leaf miner infestation in coffee crops, due to the higher value of $R^2$ and lower value of RMSE. The NDVI was the vegetation index that presented the lowest performance for estimating coffee leaf miner infestation. However, when comparing the results of October with September, all the vegetation indices presented lower performance when estimating the infestation with coffee leaf miner in October.

### *3.5. Application of the New Index for Mapping the Coffee Leaf Miner Infestation on a Regional Scale*

The map of coffee leaf miner infestation using the CLMI index and the supervised Random Forest and Support Vector Machine (SVM) algorithms on Sentinel-2A images, from 26 to 28 September 2020, in four plots in the CETP, CESP, CEMA experimental fields, and CEPC can be seen in Figure 6.

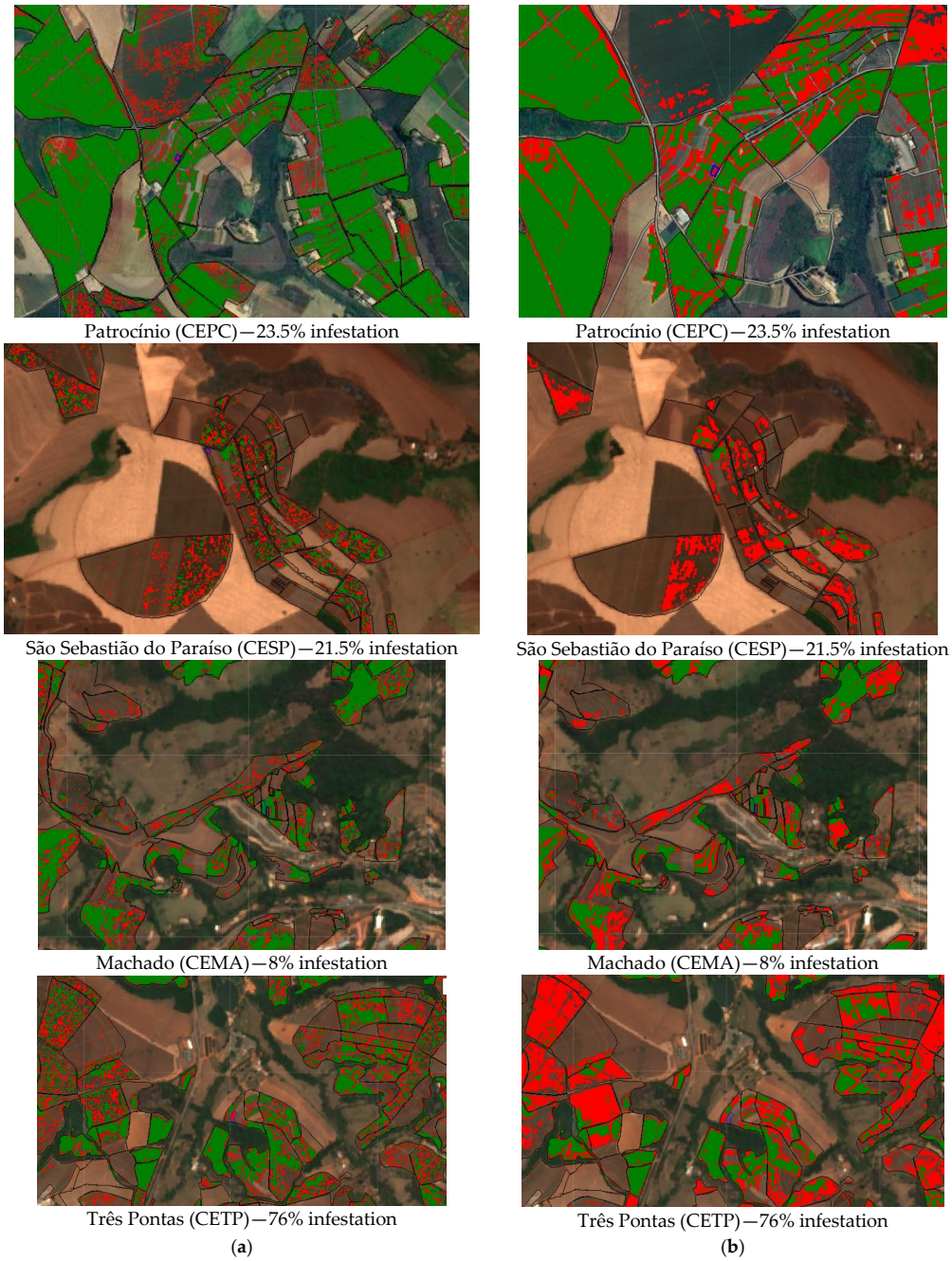


**Figure 6.** Map of coffee leaf miner infection produced by Random Forest (**a**) and SVM (**b**). The Green color shows coffee without coffee leaf miner; the Red color indicates coffee with coffee leaf miner. The Blue color shows the field where the monitoring of coffee leaf miner infestation was carried out. In black are the coffee growing areas [41].

The coffee leaf miner infestation map using the CLMI index and the supervised Random Forest algorithm showed areas with lower coffee leaf miner infestation when compared to the map that used the SVM algorithm. The Experimental Research Station of CETP and CEMA were the sites that showed the highest infestation with leaf miner (Figure 6).

The performance of the new index for monitoring coffee leaf miner infestation using Random Forest and SMV is shown in Table 7. The confusion matrix, the kappa index, and the accuracies for the performance evaluation were considered, and the type I and II errors are presented.

**Table 7.** Overall verification of the developed models of the CLMI.

| **Random Forest** | | | | | | |
|---|---|---|---|---|---|---|
| | **Healthy** | **Diseased** | **Sum** | **User Accuracy (%)** | **Overall Accuracy (%)** | **Kappa** |
| Healthy | 6 | 1 | 7 | 85.7 | | |
| Diseased | 1 | 11 | 12 | 91.7 | | |
| Sum | 7 | 12 | 15 | | | |
| Producer's accuracy (%) | 85.7 | 91.7 | | | 89.5 | 95.4 |
| Type I error (%) | 14.3 | | | | | |
| Type II error (%) | 8.3 | | | | | |
| **Support Vector Machine** | | | | | | |
| | **Healthy** | **Diseased** | **Sum** | **User Accuracy (%)** | **Overall Accuracy (%)** | **Kappa** |
| Healthy | 6 | 3 | 9 | 66.7 | | |
| Diseased | 1 | 12 | 13 | 92.3 | | |
| Sum | 7 | 15 | 22 | | | |
| Producer's accuracy (%) | 85.7 | 80.0 | | | 81.8 | 61.3 |
| Type I error (%) | 14.3 | | | | | |
| Type II error (%) | 20.0 | | | | | |

Random Forest presented the best accuracy indices and the lowest errors when compared to the values found when using the SVM algorithm to classify coffee leaf miner infestation. The Random Forest algorithm reached an overall accuracy and kappa index higher than 89%, whereas the SVM algorithm found an overall accuracy of 81.8% and a kappa of 61.3%.

## 4. Discussion

In this study, we show that coffee crops with an infestation lower than 23.5% had lower reflectances in the Blue, Green, and Red range when compared to the coffee crop with an infestation of 76%. In the visible region (Blue, Green, and Red), the reflectance in the leaves is determined by the pigments of chlorophyll (65%), carotene (6%), and xanthophylls (29%) which, when interacting with electromagnetic radiation, absorb radiation in the Blue region [42]. Therefore, the degradation of pigments (chlorophyll, carotene, and xanthophylls) because of the coffee leaf miner infestation, causes a pronounced spectral variation in the visible range, mainly in the Blue range. For the Near-Infrared range, the coffee plantation with the highest infestation of a coffee leaf miner (76%) had the lowest reflectance. Infrared reflectance can be affected by changes that occur in the leaf parenchyma [14], as the coffee leaf miner larva can penetrate the leaf mesophyll and destroy the parenchyma [4]. This phenomenon can explain the lower Near-Infrared reflectance (NIR) when there is an increase in coffee leaf miner infestation. Therefore, the Near-Infrared range can be used to assess infestations of pests that attack the internal structure of the leaf [42,43]. The CLMI was defined as the area of the triangle based on the spectral reflectance in the Blue, Red, and NIR regions.

Table 5 shows $R^2$ and RMSE values of the regression equations developed from the CLMI and the other 10 vegetation indices. It can be observed that the indices that presented the best performance were those that had the NIR, Red, and Blue bands. NDVI presented the best performance of statistical criteria ($R^2$ and RMSE) for CLMIE, followed by IPVI

and EVI. The indices that presented the bands Green, Re1, and Re2, were the indices that presented the lowest performance, such as the REIP and MTCI indices, which presented the coefficients of determination of 0.017 and 0.32, respectively. The low performance of these indices shows that the use of the Green, Re1, and Re bands of Sentinel-2 does not monitor the CLMIE. October was the month with the lowest values of $R^2$, when compared to September. The month of September is the beginning of a phenological phase of coffee; therefore, the difference between the months of September and October may be associated with the different physiological conditions between these two months.

The mapping of the area with coffee leaf miner infestation was carried out using the CLMI. The accuracy of the mapping can be seen in the confusion matrix in Table 3. The producer's accuracy shows the error of omission, reveals how much the algorithm can identify from the real data, and measures the classification accuracy; the user's accuracy shows the commission error, showing the reliability of a class corresponding to the field of truth [44]. For Random Forest, producer accuracy and user accuracy were identical and above 85% for both healthy and infested coffee. The SVM presented a lower performance than the Random Forest algorithm, but the performance of SVM was above 80% for user and producer precision for the user and producer accuracy. A type I error is a false positive, which is when it is estimated that there is an infestation with a coffee leaf miner, but in reality, there is no infestation in the field. A type II error (false negative) estimates that an infestation is not occurring, but in reality, an infestation is taking place. The Random Forest and SVM algorithms presented errors (I and II) below 20%. The kappa coefficient is a statistical method used to assess the level of agreement between two sets of data. Kappa values greater than 80% represent excellent agreement and between 60% and 80% have a substantial agreement [45]. The Random Forest algorithm presented a kappa coefficient of 95%, and the SVM presented a kappa coefficient of 61.3%. These data show that the use of Random Forest and SVM algorithms associated with the new index could identify with good accuracy the coffee leaf miner infestation in the field.

Mapping using the CLMI index through the machine learning method could be used to identify coffee crops with coffee leaf miner infestation and coffee crops without coffee leaf miner infestation based on the spectral reflectance of coffee crops. There are some limitations and challenges in monitoring coffee leaf miner infestation with CLMI on a regional scale. First, the multispectral data were taken from coffee crops at the same phenological stage, and it is not known whether the behavior of the index would be the same at other stages. Second, the management of the areas was similar in the study areas, and the management practices may be different among the producers. The new index developed can be used to aid in the remote detection of coffee leaf miner infestation on a regional scale in a fast and non-invasive way, facilitating the control of the infestation by reducing monitoring costs. Therefore, the new index can provide optimization of the use of agricultural pesticides. Monitoring of coffee leaf miner infestation at the regional level plays an important role in agriculture. This fast, non-destructive, and low-cost approach can be used as a method of monitoring the coffee leave miner infestation on a regional scale so that the rural producer can be aware of a possible increase in the infestation of the coffee leaf miner on his property. This awareness would allow the producer to increase visits in the field at the periods indicated during monitoring.

## 5. Conclusions

This study identified three bands that can best be used to identify leaf miner infestation (Blue, Red, and NIR). The new index, CLMI, was developed to detect coffee leave miner infestation. From this index, an infestation map was generated, with Random Forest being the algorithm that presented the best results. Thus, CLMI can identify coffee leaf miner infestation thanks to all the complexity involved in detecting pests via orbital remote sensing. It is understood that the improvement of the model would take place through the insertion of a greater amount of data from the infestation record. In addition, environmental conditions must also be taken into consideration, as coffee leaf miner

infestation is influenced by also close to bio-tic conditions. A limitation of this method is the reliance on clear (cloudless) environmental conditions for the location being assessed. Future studies that consider the inclusion of more variables and that take into account environmental factors should be carried out to improve the monitoring of leaf miner infestation.

**Author Contributions:** Conceptualization, E.F.V. and W.P.M.F.; methodology, E.F.V., W.P.M.F., R.A.S., I.A.L., C.d.S.M.d.M.; G.D.M.d.C., A.L.R.d.F. and D.H.L.; funding acquisition, M.V.; writing—original draft, E.F.V. and W.P.M.F.; writing—review and editing, M.V. All authors have read and agreed to the published version of the manuscript.

**Funding:** This research was funded by "Consórcio Brasileiro de Pesquisa e Desenvolvimento do Café" (CBP&D-Café), "Conselho Nacional de Desenvolvimento Científico e Tecnológico" (CNPq), and "Fundação de Amparo à Pesquisa de Minas Gerais" (FAPEMIG).

**Institutional Review Board Statement:** Not applicable.

**Data Availability Statement:** Not applicable.

**Conflicts of Interest:** The authors declare no conflict of interest. The funders had no role in the design of the study; in the collection, analyses, or interpretation of data; in the writing of the manuscript; or in the decision to publish the results.

## References

1. ICO International Coffee Organization. Historical Data on the Global Coffee Trade. Available online: http://www.ico.org/new_historical.asp (accessed on 28 June 2022).
2. CONAB Companhia Nacional de Abastecimento. Historical Series—Arabica Coffee—Brazil. Available online: https://www.conab.gov.br/info-agro/safras/serie-historica-das-safras#café-2 (accessed on 20 June 2022).
3. Silva, R.A.; Souza, J.C.; Matos, C.S.M.; Pereira, A.B. *Bicho-Mineiro do Cafeeiro*; EPAMIG: Belo Horizonte, Brazil, 2022.
4. Dantas, J.; Motta, I.O.; Vidal, L.A.; Nascimento, E.F.M.B.; Bilio, J.; Pupe, J.M.; Veiga, A.; Carvalho, C.; Lopes, R.B.; Rocha, T.L.; et al. A Comprehensive Review of the Coffee Leaf Miner *Leucoptera coffeella* (Lepidoptera: Lyonetiidae)—A Major Pest for the Coffee Crop in Brazil and Others Neotropical Countries. *Insects* **2021**, *12*, 1130. [CrossRef] [PubMed]
5. Reis, P.R.; Souza, J.C.; Silva, R.A.; Santa-Cecília, L.V.C. Principais pragas do cafeeiro no Cerrado Mineiro: Reconhecimento e manejo. In *Cafeicutura do Cerrado*; Carvalho, G.R., Ferreira, A.D., Andrade, V.T., Botelho, C.E., Carvalho, J.P.F., Eds.; EPAMIG: Belo Horizonte, Brazil, 2021; p. 564.
6. Souza, J.C.; Reis, P.R.; Rigitano, R.L.O. *Bicho-Mineiro Do Cafeeiro: Biologia, Danos e Manejo Integrado*; EPAMIG: Belo Horizonte, Brazil, 1998.
7. Cure, J.R.; Rodríguez, D.; Gutierrez, P.A.; Point, L. The Coffee Agroecosystem: Bio-Economic Analysis of Coffee Berry Borer Control (*Hypothenemus hampei*). *Sci. Rep.* **2020**, *10*, 12262. [CrossRef]
8. Venzon, M. Agro-ecological Management of Coffee Pests in Brazil. *Front. Sustain. Food Syst.* **2021**, *5*, 721117. [CrossRef]
9. de Oliveira Aparecido, L.E.; Lorençone, P.A.; Lorençone, J.A.; de Meneses, K.C.; de Lima, R.F.; da Silva Cabral Moraes, J.R.; Torsoni, G.B. Coffee Pest Severity by Agrometeorological Models in Subtropical Climate. *Int. J. Biometeorol.* **2022**, *66*, 957–969. [CrossRef]
10. Reis, P.R.; Souza, J.C.; Santa-Cecília, L.V.C.; Silva, R.A.; Zacarias, M.S. Manejo integrado das pragas do cafeeiro. In *Café Arábia do Plantio à Colheita*; Reis, P.R., Cunha, R.L., Eds.; EPAMIG: Lavras, Brazil, 2010; Volume 1, 896p.
11. Liu, L.; Dong, Y.; Huang, W.; Du, X.; Ren, B.; Huang, L.; Zheng, Q.; Ma, H. A Disease Index for Efficiently detecting Wheat Fusarium Head Blight using Sentinel-2 Multispectral Imagery. *IEEE Access* **2020**, *8*, 52181–52191. [CrossRef]
12. Prabhakar, M.; Gopinath, K.A.; Kumar, N.R.; Thirupathi, M.; Sravan, U.S.; Kumar, G.S.; Siva, G.S.; Meghalakshmi, G.; Vennila, S. Detecting the Invasive fall Armyworm Pest Incidence in Farm Fields of Southern India using Sentinel-2A Satellite Data. *Geocarto Int.* **2021**, *37*, 3801–3816. [CrossRef]
13. Ramos, A.P.M.; Gomes, F.D.G.; Pinheiro, M.M.F.; Furuya, D.E.G.; Gonçalvez, W.N.; Junior, J.M.; Michereff, M.F.F.; Blassioli-Moraes, M.C.; Borges, M.; Alaumann, R.A.; et al. Detecting the Attack of the Fall Armyworm (Spodoptera frugiperda) in Cotton Plants with Machine Learning and Spectral Measurements. *Precis. Agric.* **2022**, *23*, 470–491. [CrossRef]
14. Ponzoni, F.J.; Shimabukuro, Y.E.; Kuplich, T.M. *Sensoriamento Remoto Aplicado ao Estudo da Vegetação*, 2nd ed.; Parêntese: São José dos Campos, Brazil, 2012; 160p.
15. Tamiminia, H.; Salehi, B.; Mahdianpari, M.; Quackenbush, L.; Adeli, S.; Brisco, B. Google Earth Engine for Geo-big Data Applications: A Meta-Analysis and Systematic Review. *ISPRS J. Photogramm. Remote Sens.* **2020**, *164*, 152–170. [CrossRef]
16. Amani, M.; Ghorbanian, A.; Ahmadi, S.A.; Kakooei, M.; Moghimi, A.; Mirmazloumi, S.M.; Moghaddam, S.H.A.; Mahdavi, S.; Ghahremanloo, M.; Parsian, S.; et al. Google Earth Engine Cloud Computing Platform for Remote Sensing Big Data Applications: A Comprehensive Review. *IEEE J. Sel. Top. Appl. Earth Obs. Remote Sens.* **2020**, *13*, 5326–5350. [CrossRef]

17. Buchaillot, M.L.; Cairns, J.; Hamadziripi, E.; Wilson, K.; Hughes, D.; Chelal, J.; McCloskey, P.; Kehs, A.; Clinton, N.; Araus, L.J.; et al. Regional Monitoring of Fall Armyworm (FAW) Using Early Warning Systems. *Remote Sens.* **2022**, *14*, 5003. [CrossRef]
18. Cao, J.; Zhao, Z.; Liangliang, Z.; Yuchuan, L.; Ziyue, L.; Fulu, T. Damage Evaluation of Soybean Chilling Injury Based on Google Earth Engine (GEE) and Crop Modelling. *J. Geogr. Sci.* **2020**, *30*, 1249–1265. [CrossRef]
19. ESA European Space Agency. Sentinel-2 User Handbook. Available online: https://sentinel.esa.int/documents/247904/685211/Sentinel-2_User_Handbook (accessed on 17 November 2019).
20. Kumar, V.; Ramachandran, D.; Kumar, B. Influence of New-age Technologies on Marketing: A Research Agenda. *J. Bus. Res.* **2021**, *125*, 864–877. [CrossRef]
21. Chemura, A.; Mutanga, O.; Dube, T. Separability of Coffee Leaf Rust Infection Levels with Machine Learning Methods at Sentinel-2 MSI Spectral Resolutions. *Precis. Agric.* **2017**, *18*, 859–881. [CrossRef]
22. Zheng, Q.; Huang, W.; Cui, X.; Shi, Y.; Liu, L. New Spectral Index for Detecting Wheat Yellow Rust Using Sentinel-2 Multispectral Imagery. *Sensors* **2018**, *18*, 868. [CrossRef] [PubMed]
23. Marin, D.B.; Feraaz, S.A.G.; Santana, L.S.; Barbosa, B.D.S.; Barata, R.A.P.; Osco, L.P.; Ramos, A.P.M.; Guimarães, P.H.S. Detecting Coffee Leaf Rust with UAV-based Vegetation Indices and Decision Tree Machine Learning Models. *Comput. Electron. Agric.* **2021**, *190*, 106476. [CrossRef]
24. Marin, D.B.; Ferraz, G.A.S.; Schwerz, F.; Barata, R.A.P.; Faria, R.d.O.; Dias, J.E.L. Unmanned Aerial Vehicle to Evaluate Frost Damage in Coffee Plants. *Precis. Agric.* **2021**, *22*, 1845–1860. [CrossRef]
25. Funk, C.; Peterson, P.; Landsfeld, M.; Pedreros, D.; Verdin, J.; Shukla, S.; Husak, G.; Rowland, J.; Harrison, L.; Hoell, A.; et al. The Climate Hazards Infrared Precipitation with Stations—A New Environmental Record for Monitoring Extremes. *Sci. Data* **2015**, *2*, 150066. [CrossRef] [PubMed]
26. Copernicus Climate Change Service (C3S). ERA5: Fifth Generation of ECMWF Atmospheric Reanalyses of the Global Climate. *Copernicus Climate Change Service Climate Data Store (CDS)*. 2017. Available online: https://cds.climate.copernicus.eu/cdsapp#!/home (accessed on 10 May 2022).
27. Jordan, C.F. Derivation of Leaf Area Index from Quality of Light on the Forest Floor. *Ecology* **1969**, *50*, 663–666. [CrossRef]
28. Richardson, A.J.; Wiegand, C.L. Distinguishing Vegetation from Soil Background Information. *Photogramm. Eng. Remote Sens.* **1977**, *43*, 1541–1552.
29. R Development Core Team. In *R: A Language and Environment for Statistical Computing*; R Foundation for Statistical Computing: Vienna, Austria, 2022.
30. Rouse, J.W., Jr.; Haas, R.H.; Schell, J.A.; Deering, D.W. Monitoring vegetation systems in the great plains with ERTS. *NASA Spec. Publ.* **1974**, *351*, 309.
31. Justice, C.O.; Vermote, E.; Townshend, J.R.; Defries, R.; Roy, D.P.; Hall, D.K.; Salomonson, V.V.; Privette, J.L.; Riggs, G.; Strahler, W.; et al. The Moderate Resolution Imaging Spectroradiometer (MODIS): Land Remote Sensing for Global Change Research. *IEEE Trans. Geosci. Remote Sens.* **1998**, *36*, 1228–1249. [CrossRef]
32. Gitelson, A.A.; Kaufman, Y.J.; Merzlyak, M.N. Use of a green channel in remote sensing of global vegetation from EOS-MODIS. *Remote Sens. Environ.* **1996**, *58*, 289–298. [CrossRef]
33. Crippen, R. Calculating the Vegetation Index Faster. *Remote Sens. Environ.* **1990**, *34*, 71–73. [CrossRef]
34. Daughtry, C.S.T.; Walthall, C.L.; Kim, M.S.; de Colstoun, E.B.; McMurtrey, J.E. Estimating Corn Leaf Chlorophyll Concentration from Leaf and Canopy Reflectance. *Remote Sens. Environ.* **2000**, *74*, 229–239. [CrossRef]
35. Dash, J.; Curran, P.J. The Meris Terrestrial Chlorophyll Index. *Int. J. Remote Sens.* **2004**, *25*, 5403–5413. [CrossRef]
36. Guyot, G.; Baret, F.; Major, D.J. High Spectral Resolution: Determination of Spectral Shifts between the Red and Infrared. *Int. Arch. Photogramm. Remote Sens.* **1988**, *11*, 750–760.
37. Fernández-Manso, A.; Fernández-Manso, O.; Quintano, C. Sentinel-2A Red-Edge Spectral Indices Suitability for Discriminating Burn Severity. *Int. J. Appl. Earth Obs. Geoinf.* **2016**, *50*, 170–175. [CrossRef]
38. Roujean, J.L.; Breon, F.M. Estimating PAR Absorbed by Vegetation from Bidirectional Reflectance Measurements. *Remote Sens. Environ.* **1995**, *51*, 375–384. [CrossRef]
39. Sheykhmousa, M.; Mahdianpari, M.; Ghanbari, H.; Mohammadimanesh, F.; Ghamisi, P.; Member, S.; Homayouni, S. Support Vector Machine Versus Random Forest for Remote Sensing Image Classification: A meta-analysis and Systematic Review. *IEEE J. Sel. Top. Appl. Earth Obs. Remote Sens.* **2020**, *13*, 6308–6325. [CrossRef]
40. Fletcher, R.S.; Reddy, K.N. Random Forest and Leaf Multispectral Reflectance Data to Differentiate Three Soybean Varieties From Two Pigweeds. *Comput. Electron. Agric.* **2016**, *128*, 199–206. [CrossRef]
41. CONAB Companhia Nacional de Abastecimento. Portal de Informações Agropecuárias. In *Mapeamentos. Café-MG.2017.*. Available online: https://portaldeinformacoes.conab.gov.br/mapeamentos-agricolas-downloads.html (accessed on 15 May 2022).
42. Almeida, K.E.C.; de Souza, T.T.C.; da Costa, A.L.; Marcelo, A.S.D.S.; de Laia, L. Near-infrared Spectroscopy for the Evaluation and Prediction of Injuries Associated with the Attack of *Thaumastocoris Peregrinus* (Carpintero & Dellapé) in Eucalyptus Camaldulensis (Dehnh) Espectroscopia de Infravermelho próximo para a Avaliação e Predição de Injúrias associadas ao Ataque de Thaumastocoris Peregrinus. *Sci. For.* **2018**, *46*, 9–16. [CrossRef]
43. Kolling, B.J. Espectroscopia de Refletância Difusa para Detectação do dano Causado por Spodoptera Eridania (Cramer) (Lepidoptera: Noctuidae) na Cultura de Repolho. 2019. Available online: https://repositorio.ufsc.br/bitstream/handle/123456789/197662/BENNO%20JOSE%20KOLLING.pdf?sequence=1&isAllowed=y (accessed on 20 June 2022).

44. Congalton, R.G. A review of Assessing the Accuracy of Classifications of Remotely Sensed Data. *Remote Sens. Environ.* **1991**, *37*, 35–46. [CrossRef]
45. Landis, J.R.; Koch, G.G. The Measurement of Observer Agreement for Categorical Data. *Biometrics* **1977**, *33*, 159–174. [CrossRef] [PubMed]